PHYSICAL REVIEW C VOLUME 25, NUMBER 4 APRIL 1982

Spin observables in low energy nucleon-antinucleon scattering

C. B. Dover and J. M. Richard*
Brookhaven National Laboratory, Upton, New York 11973
(Received 23 October 1981)

We discuss the model dependence of the spin parameters for low and medium energy antinucleon-nucleon ($\bar{N}N$) scattering. An $\bar{N}N$ potential model is used, consisting of a t-channel meson exchange part, supplemented by a complex annihilation potential, adjusted to reproduce the observed energy dependence of total elastic, inelastic, and charge exchange cross sections. A number of striking spin effects are predicted, particularly in the charge exchange channel. We explore the sensitivity of the effects to changes in the real and imaginary parts of the $\bar{N}N$ potential; in particular, we assess the possibility of extracting the strength of the *coherent* $\bar{N}N$ tensor potential due to π, ρ, and ω exchange from future data. Some implications of our results for future experiments are mentioned.

[NUCLEAR REACTIONS Nucleon-antinucleon scattering, spin-dependent observables.]

I. INTRODUCTION

Except for some rather crude $\bar{p}p$ polarization measurements at a few low energies,[1] there is very little experimental data on the spin dependence of the antinucleon-nucleon ($\bar{N}N$) interaction, in contrast to the situation for the NN system, where the spin effects are well mapped out. Apart from a few angular distributions,[2] most of the available $\bar{N}N$ data involve integrated elastic cross sections[3] which can be reasonably well fitted by very crude models, such as a boundary condition[4] or black sphere model (see, e.g., Fig. 7 in Ref. 5). Total absorption cross sections can even be accounted for in terms of a purely imaginary potential, so such data do not provide a sensitive test of the Yukawa theory for the long range real part of the $\bar{N}N$ interaction. Angular distributions, especially for $\bar{p}p \to \bar{n}n$ charge exchange, depend, of course, much more on the meson-exchange tail, particularly the one pion exchange part. They, however, do not sensitively test the characteristic spin dependence (particularly tensor forces due to $\pi\pi$ and ω exchanges) of this part of the interaction. We indicate here that certain $\bar{N}N$ spin observables are in fact very sensitive to such details of the interaction and promise to provide useful constraints on models of the $\bar{N}N$ interaction.

The LEAR facility[6] at CERN, which will deliver high quality intense antinucleon beams at low energies, promises to greatly expand our empirical knowledge of the $\bar{N}N$ interaction. In particular, experiments to measure $\bar{N}N$ spin dependent observables should become possible in the near future. It thus seems appropriate to examine some models for the $\bar{N}N$ interaction in order to see what sort of spin effects may be anticipated, and how they may reveal interesting details of the spin structure of the $\bar{N}N$ potential. We emphasize here the qualitative features; the detailed predictions will of course change as the models are refined. Our observations may be of some interest in planning future experiments at LEAR.

In Sec. II, we present a brief review of the potential model employed to describe the $\bar{N}N$ interaction, as well as the formalism pertinent to the $\bar{N}N$ spin observables. In Sec. III, we discuss selected numerical results based on a potential model[7] for the $\bar{N}N$ interaction, adjusted to fit the observed energy dependence of total elastic, and charge exchange cross sections.

II. THE $\bar{N}N$ POTENTIAL AND SPIN OBSERVABLES

To describe the $\bar{N}N$ interaction arising from meson exchange (t channel), we start with the Paris[7] model for the NN potential, and use the G-parity transformation to relate the NN and $\bar{N}N$ potentials (sign change for $G=-1$ exchanges such as π and ω). This provides a model for the medium and long

range parts of the potential of the form ($r \geq r_0$)

$$V_t^{NN}(r) = V_\pi(r) + V_{2\pi}(r) + V_\omega(r) ,$$
$$V_t^{\bar{N}N}(r) = -V_\pi(r) + V_{2\pi}(r) - V_\omega(r) . \quad (2.1)$$

In the Paris model,[8] the two pion exchange piece $V_{2\pi}(r)$ [which includes the ρ and ϵ contributions of more phenomenological one boson exchange (OBE) models] is calculated in a dispersion theory approach, using πN and $\pi\pi$ scattering data as input. The details of the Paris potential are discussed in Refs. 7 and 8, and its implications for the $\bar{N}N$ interaction in Refs. 5 and 9. The behavior of the real $\bar{N}N$ potential at short distances is essentially unknown theoretically, and is largely unconstrained by the existing $\bar{N}N$ scattering data. We have chosen a square well cutoff $V_{\bar{N}N}(r) = V_{\bar{N}N}(r_0)$ for $r \leq r_0 = 0.8$ fm as in Ref. 10.

The real potential $V_t^{\bar{N}N}$ from meson exchange must be supplemented by a short range part $V_{\rm SR}$ accounting for elastic forces in the core region and annihilation into mesons. There have been several recent attempts to derive the $\bar{N}N$ annihilation potential. Some groups[11] still consider as a guide s-channel meson exchange diagrams, as in the early paper of Martin.[12] In this approach, mesons and nucleons are treated as elementary objects. One can also try to understand $\bar{N}N$ annihilation in terms of processes involving quarks. Maruyama and Ueda,[13] for instance, build their model from the assumption of a simple rearrangement of the quarks and antiquarks. We note that in this approximation no $K\bar{K}$ pairs would be produced, contrary to experiment. In Ref. 14, the driving process is a quark-antiquark annihilation into one gluon. The rearrangement of the gluon and the remaining quarks into a physical state is not considered. Also the relevance of perturbative quantum chromodynamics (QCD) for such a process is not demonstrated. In this paper, we adopt, as in Ref. 10, a purely phenomenological form for $V_{\rm SR}$

$$V_{\rm SR}(r) = -(V_0 + iW_0)/(1 + e^{(r-R)/a}) . \quad (2.2)$$

The parameters V_0, W_0, R, and a can be determined by a fit to total cross section data (elastic, inelastic, and charge exchange). One of our goals here is to test the sensitivity of the $\bar{N}N$ spin observables to the parameters of the absorptive potential. Accordingly, we consider two models which produce essentially the same quality of fit to total cross section data. Model I is taken from Ref. 10, and consists of the choice

$$R = 0, \quad a = \tfrac{1}{5} \text{ fm}, \quad V_0 = 21 \text{ GeV}, \quad W_0 = 20 \text{ GeV}$$
(model I) . (2.3)

A second model is obtained by allowing $V_{\rm SR}(r)$ to have a flat region for small r (i.e., $R \neq 0$) and readjusting W_0 and V_0 to obtain about the same strength in the region near $r \approx 1.1$ fm. This leads to

$$R = 0.8 \text{ fm}, \quad a = \tfrac{1}{5} \text{ fm}, \quad V_0 = 500 \text{ MeV} ,$$
$$W_0 = 500 \text{ MeV}$$
(model II) . (2.4)

Model II corresponds to weaker absorption in the far surface region ($r > 1.5$ fm). As we shall see, spin observables (which can depend on delicate interferences between different amplitudes) are more sensitive to this region than total cross sections. Note that both models I and II include a real part for $V_{\rm SR}(r)$; the fit[10] to total cross sections displays a preference for an attraction comparable in size to the imaginary part. Our $V_{\rm SR}(r)$ is independent of spin S, isospin I, and energy E. A more extensive fit to $\bar{N}N$ data by Vinh Mau and collaborators[11] indicates the need for departures from our simplified picture. The strong dependence on S, I, and E that they find must also exert a significant influence on the spin observables.

The general features of $\bar{N}N$ potentials have been reviewed in Refs. 5 and 9. The most striking feature of $V_t^{\bar{N}N}(r)$, which is characteristic of any meson exchange model, is the *coherence* of tensor [$V_T(r)$] and quadratic spin-orbit [$V_{LS2}(r)$] potentials for isospin $I = 0$. That is, the contributions to $V_T(r)$ generated by π, ρ, and ω exchange are all of the *same sign* for $I = 0$, leading to repulsion for $J = L$ and attraction for $J = L \pm 1$. On the other hand, the $\vec{L}\cdot\vec{S}$ and $\vec{\sigma}_1\cdot\vec{\sigma}_2$ potentials do not display such coherence for $\bar{N}N$, in contrast to the situation for NN, where coherent repulsion of spin-orbit potentials[5] leads to a zero in the $^3P_0$ phase shift, for instance. The $\bar{N}N$ and NN systems are thus primarily sensitive to different components of the underlying potential. Our hope is that the $\bar{N}N$ spin observables will enable us to determine the summed strength of the tensor interaction. Clearly, the pion tensor force has the most important influence on spin properties, because of its long range. It will be interesting to see to what extent one can extract the coherent vector meson contribution, in the presence of a rather strong absorptive potential. We are also interested in isolating dramatic spin effects which are relatively model independent, i.e., driven essentially by pion exchange alone. That is, we look for

situations where one obtains large polarizations, depolarizations, spin rotations, etc. Such observations could be of interest for the design of polarized beams at LEAR.

The spin formalism for the analysis of nucleon-nucleon scattering experiments has been given in detail in the literature.[15,16] We have evaluated all the spin observables (except for third and fourth rank spin correlation tensors) for the three reactions $\bar{p}p \to \bar{p}p$, $\bar{p}n \to \bar{p}n$, and $\bar{p}p \to \bar{n}n$, using both the formalisms of Hoshizaki[15] and Bystricky, Lehar, and Winternitz.[16] These two approaches, which use different representations for the amplitudes, were used independently to provide a numerical check on the calculation. We use the norelativistic expressions for spin observables in the laboratory system (Table V of Hoshizaki[15]). With the exception of a sign error for A_t and A_t' in Ref. 15 (and unfortunately forwarded in Ref. 17), the two approaches were consistent.

Note that there are some important differences between the symmetry properties of NN and $\bar{N}N$ observables. For $\bar{N}N$, the Pauli principle no longer operates, so for each partial wave L, all four spin-isospin combinations ($S=0,1$ and $I=0,1$) are allowed. Symmetries of the spin observables due to the transformation $\theta \leftrightarrow \pi - \theta$ are no longer satisfied for the $\bar{N}N$ system. However, there are still five complex amplitudes as for NN scattering. An antisymmetric spin-orbit term proportional to $(\vec{\sigma}_1 - \vec{\sigma}_2)\cdot\vec{L}$, which occurs in the ΛN potential, for instance, is absent for $\bar{N}N$ due to G-parity conservation.

The potential models outlined above have been used to compute the difference of cross sections

$$\Delta\sigma_L = \sigma_{\rightleftarrows} - \sigma_{\rightrightarrows}\,, \qquad \Delta\sigma_T = \sigma_{\downarrow\uparrow} - \sigma_{\uparrow\uparrow}\,, \tag{2.5}$$

as well as the spin tensors of rank one and two, i.e., the polarization P, the depolarization D, the spin-rotation parameters $A,A'R,R'$, the polarization transfers D_t,A_t,R_t,R_t', and the spin correlation tensors A_{ij} and C_{ij}. The notation is that of Hoshizaki,[15] to which we refer the reader for further details.

III. RESULTS AND PREDICTIONS

It is essentially impossible to display any sizable fraction of our results in detail. In any case, this is hardly appropriate, since except for $P(\theta)$, no experimental data exists. We restrict ourselves to a qualitative survey, emphasizing some of the more striking spin effects. Detailed predictions for any quantity may be obtained from the authors upon request.

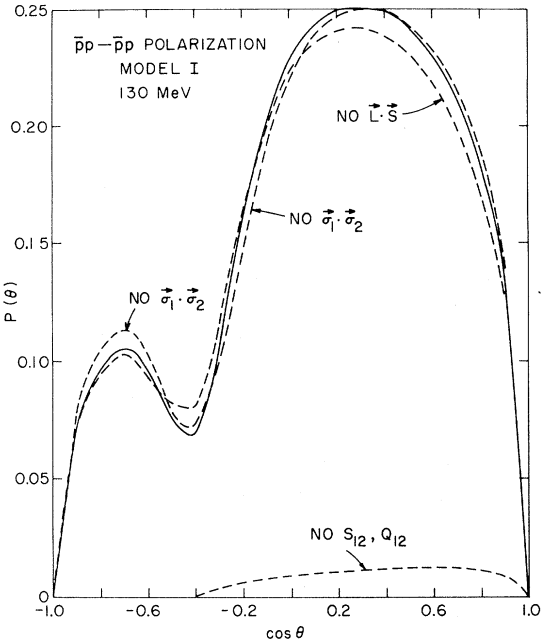

FIG. 1. Elastic $\bar{p}p \to \bar{p}p$ polarization $P(\theta)$ in model I at a laboratory kinetic energy of 130 MeV, as a function of $\cos\theta$ (θ=laboratory scattering angle). The solid curve is the exact result, while the dashed curves show the effect of omitting spin-orbit ($\vec{L}\cdot\vec{S}$), spin-spin ($\vec{\sigma}_1\cdot\vec{\sigma}_2$), or tensor and quadratic spin-orbit (S_{12},Q_{12}) components of the meson exchange potential.

As expected from the coherence argument outlined in Sec. II, tensor forces play the dominant role

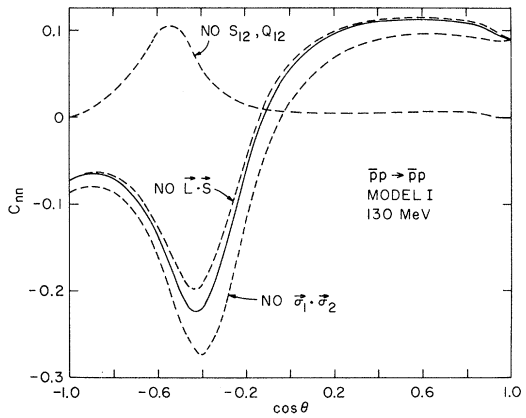

FIG. 2. Spin-spin correlation coefficient C_{nn} for $\bar{p}p \to \bar{p}p$ at 130 MeV in model I. The solid curve incorporates the full potential while the dashed curves indicate the effect of omitting various parts of the spin-dependent potential, as in Fig. 1.

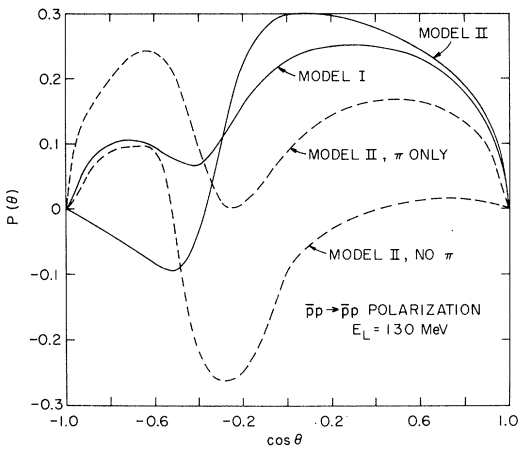

FIG. 3. Model dependence of the $\bar{p}p \to \bar{p}p$ elastic polarization $P(\theta)$ at 130 MeV. Keeping the meson exchange potential fixed, the two solid curves show the effect of changing the annihilation potential (model I vs model II). For model II, we also show the effect of omitting two and three pion exchanges (π only), or omitting the one pion exchange contribution while retaining heavier meson exchanges (no π).

in producing sizable spin effects in the $\bar{N}N$ system. The effect of $\vec{L}\cdot\vec{S}$ and $\vec{\sigma}_1\cdot\vec{\sigma}_2$ terms is found to be quite small. We illustrate this point in Figs. 1 and 2 for $P(\theta)$ and $C_{nn}(\theta)$ at 130 MeV. The dashed curves indicate the effect of turning off various pieces of the $\bar{N}N$ potential, leaving $V_{\rm SR}(r)$ fixed. The neglect of spin-orbit and spin-spin terms has only a small effect on the angular shape. Neglecting coherent tensor and quadratic spin-orbit terms,

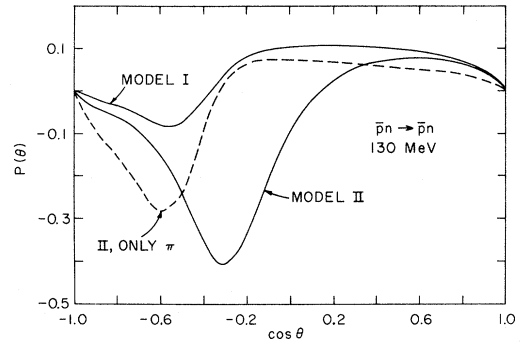

FIG. 4. Model dependence of the isospin $I=1$ polarization ($\bar{p}n \to \bar{p}n$ or $\bar{n}p \to \bar{n}p$) at 130 MeV. The effect of omitting two and three pion exchanges is indicated by the dashed line. The solid curves include the full meson exchange potential, but vary the annihilation potential. A comparison of Figs. 3 and 4 reveals the effect of the strong isospin dependence of the meson exchange potential (the absorptive part is taken to be isospin independent).

however, produces a drastic change. Without these terms, almost no $\bar{p}p \to \bar{p}p$ polarization is obtained. Note that $V_T(r)$ is much more important than $V_{LS2}(r)$, due to the key role of pion exchange, which does not generate spin-orbit terms. This is in striking contrast to the situation for the NN case, where $P(\theta)$ arises mostly from spin orbit rather than tensor effects. It is clear that we are looking at complementary aspects of meson exchange potentials in NN and $\bar{N}N$ spin observables.

The model dependence of our results for the polarization $P(\theta)$ for $\bar{p}p \to \bar{p}p$ and $\bar{p}n \to \bar{p}n$ (or $\bar{n}p \to \bar{n}p$) is shown in Figs. 3 and 4. The sensitivity to the absorptive potential (model I vs model II) is quite noticeable, particularly in the backward hemisphere ($\cos\theta < 0$). Model II, corresponding to weaker absorption, leads to larger polarizations in general than model I; this holds also for most other spin observables. The available data[3] for $P(\theta)$ are restricted to the forward hemisphere and have large error bars; they are consistent with both models I and II. Note that $P(\theta)$ remains rather small at all angles, not exceeding about 0.3 in magnitude (unless the absorptive potential is weakened further). Even at lower energies in the range 30—100 MeV, the peak $\bar{p}p \to \bar{p}p$ polarization does not exceed about 0.3 or so. The effect of removing various components of the real potential is also shown in Figs. 3 and 4. If the π exchange potential is neglected, the predictions for $P(\theta)$, as well as most other spin observables, change qualitatively; the effect is much more modest for total cross sections. If the pion is retained, but $V_{2\pi}$ and V_ω are neglected, the effect is less dramatic than for $V_\pi = 0$, but still quite noticeable, particularly for large angles. In an eventual

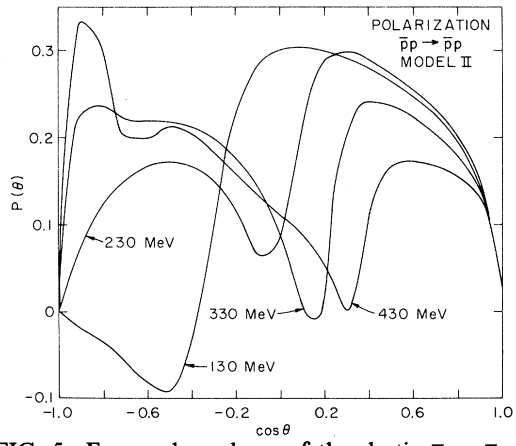

FIG. 5. Energy dependence of the elastic $\bar{p}p \to \bar{p}p$ polarization in model II. The curves are labeled by the laboratory kinetic energy.

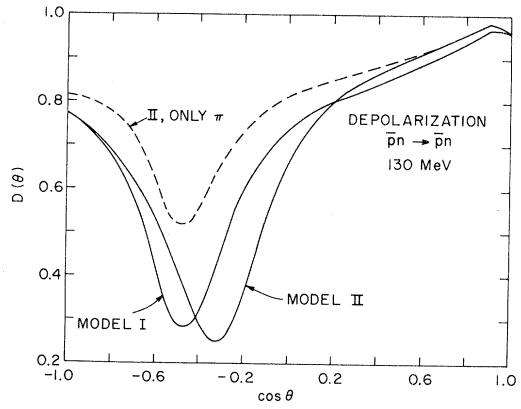

FIG. 6. Depolarization parameter $D(\theta)$ for $I=1$ at 130 MeV. The solid curves correspond to choosing model I or II for the annihilation potential. The dashed curve shows the effect of omitting $\pi\pi$ and ω exchange in model II.

analysis of data, the difficulty in isolating the interesting effects of scalar and vector meson exchange will be in distinguishing them from changes induced by varying the short range core. As seen in Fig. 4, for instance, changes in $V_{SR}(r)$ can mimic the effect of $V_{2\pi}$ and V_{ω}. The untangling of these effects must consider the energy dependence of a number of spin quantities. The predicted energy dependence of $P(\theta)$ for $\bar{p}p \to \bar{p}p$ is shown in Fig. 5. For $\cos\theta > 0$, the polarization evolves in a very smooth fashion as the energy increases. Larger peak polarizations are obtained at lower energy. For $\cos\theta < 0$, very rapid energy dependences are anticipated, the details of which are sensitive to the model for $V_{SR}(r)$.

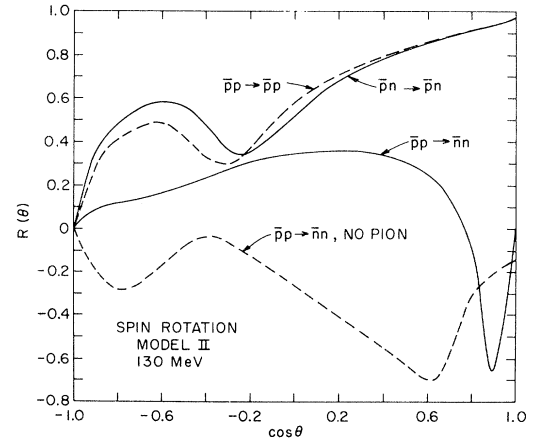

FIG. 7. Isospin dependence of the spin rotation parameter $R(\theta)$ in model II at 130 MeV. For $\bar{p}p \to \bar{n}n$ charge exchange, the influence of the one pion exchange is also shown.

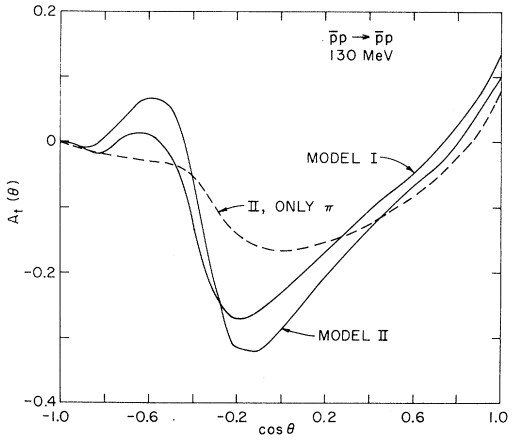

FIG. 8. Polarization transfer $A_t(\theta)$ for elastic scattering at 130 MeV.

Several other observables display more dramatic spin effects than $P(\theta)$, although they are also more difficult to measure. For instance, we display the depolarization $D(\theta)$ for $\bar{p}n \to \bar{p}n$ at 130 MeV in Fig. 6. A very small value of $D(\theta)$ is predicted for $\cos\theta \approx -0.4$ [recall $D(\theta)=1$ in the absence of spin dependence]. The size of this effect depends strongly on the 2π and ω contribution. Since models I and II give rather similar predictions, this may afford a good probe of the strength of the coherent tensor potential.

In Fig. 7, we give an example of the strong isospin dependence of spin observables, by plotting the spin rotation parameter $R(\theta)$ for $\bar{p}n \to \bar{p}n$ (pure $I=1$ in s channel), $\bar{p}p \to \bar{p}p$ (mixture of $I=0,1$ both in s and t channels), and $\bar{p}p \to \bar{n}n$ $I=0,1$ in s channel, $T=1$ in t channel). The dominant role of pion exchange in the charge exchange process is indicated by the dashed line in Fig. 7, which shows the drastic consequence of omitting V_{π}. Note that very large values of $R(\theta)$, of either sign depending on the channel, can be expected.

In Fig. 8, we display the polarization transfer $A_t(\theta)$ for $\bar{p}p \to \bar{p}p$ at 130 MeV. As for $D(\theta)$, the 2π and ω exchanges, through their coherent tensor potential, serve to amplify the size of $A_t(\theta)$. Finally, in Fig. 9, we exhibit the spin correlation tensor A_{zz} for $\bar{p}p \to \bar{n}n$. It provides an example of a number of very dramatic spin dependences predicted in the charge exchange channel. The extreme variation in A_{zz} from essentially -1 to $+1$ near the forward direction is almost model independent. If tensor forces are suppressed, this effect disappears, as indicated by the dashed line in Fig. 9. In charge ex-

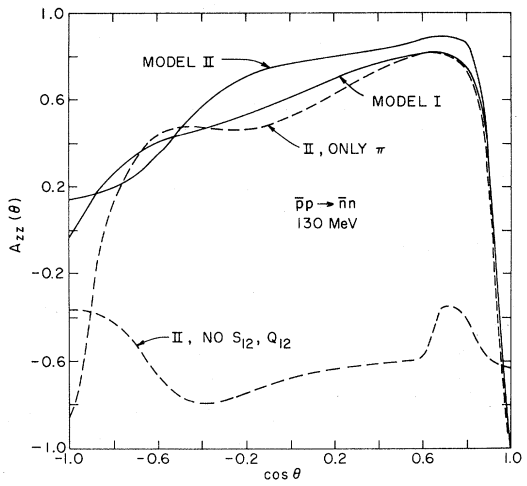

FIG. 9. Spin correlation tensor $A_{zz}(\theta)$ for $\bar{p}p \to \bar{n}n$ charge exchange at 130 MeV. Note the strong effect of omitting tensor and quadratic spin-orbit terms (S_{12}, Q_{12}). The sharp variation of $A_{zz}(\theta)$ near $\theta \approx 0$ is seen to arise dominantly from single pion exchange.

change, there are a number of observables where a very rapid angular variation is induced by pion exchange, relatively unmasked by the effects of annihilation. In addition to the example of Fig. 9, some other striking results (model I) for $\bar{p}p \to \bar{n}n$ are the following[17]:

$$\Delta\sigma_L/\sigma \approx -115\% , \tag{3.1a}$$

$$D(180°) \approx -75\% , \tag{3.1b}$$

$$A'(0°) \approx -85\% , \tag{3.1c}$$

$$A_t(0°) \approx +90\% . \tag{3.1d}$$

The large value of $\Delta\sigma_L/\sigma$ (which implies $\sigma_{\rightarrow} \approx 3\sigma_{\rightleftarrows}$ for $\bar{p}p \to \bar{n}n$!) could be checked in an experiment with a polarized $\bar{p}$ beam and a polarized hydrogen jet target (PHJT), as has been proposed[18,19] at LEAR. In other channels, the integrated cross sections are not so dramatically spin dependent. For $\bar{p}n \to \bar{p}n$, we find $\Delta\sigma_L/\sigma \approx -20\%$ and $\Delta\sigma_T/\sigma \approx 5-10\%$ for both elastic and inelastic cross sections. For $\bar{p}p \to \bar{p}p$, the result is $\Delta\sigma_L/\sigma \approx -10\%$ and $\Delta\sigma_T/\sigma \approx -7\%$ (all for model I at 130 MeV). According to Eq. (3.1c), a charge exchange experiment with an unpolarized $\bar{p}$ beam leads to strongly polarized antineutrons. The very strong spin dependences predicted in Eq. (3.1), which survive both in models I and II, thus suggest a means of producing polarized $\bar{n}$ beams.[17–19] It should be noted that our model gives a good account of the existing $\bar{p}p \to \bar{n}n$ data; in particular, the dip-bump structure observed[20] in the angular distribution at 250 MeV is well reproduced. We also observe that the process $\bar{p}p \to \bar{\Lambda}\Lambda$ is rather analogous to $\bar{p}p \to \bar{n}n$, except that K and K^* exchange replace π and ρ. Here, we also except strong coherent tensor force effects, and a fairly strong spin dependence. Indeed, existing data[21] at 6 GeV/c provide evidence for sizable polarization of the outgoing hyperons. A measurementof $\bar{p}p \to \bar{\Lambda}\Lambda$ at lower energies has been proposed.[22]

IV. CONCLUSIONS AND OUTLOOK

We have studied the spin parameters of low to medium energy nucleon-antinucleon scattering. A number of dramatic spin effects are predicted, particularly in the $\bar{p}p \to \bar{n}n$ channel. We have explored the sensitivity of these phenomena to changes in the annihilation and meson exchange potentials, using models which fit total cross section data. The heavy meson exchanges and the one pion tail are crucial in producing the rapid spin dependences, unlike the situation for total absorption cross sections. The *coherent* tensor potential due to π, ρ, and ω exchange dominates the spin effects in $\bar{N}N$ scattering; spin orbit and spin-spin forces play a relatively minor role. A careful measurement of $\bar{N}N$ spin observables would provide a constraint on the strength of the various Yukawa couplings in a meson exchange model. This constraint, which involves the summed strength of the π, ρ, and ω tensor potentials, is somewhat complementary to the information gleaned from a study of spin dependence in NN scattering, where $\vec{L}\cdot\vec{S}$ and $\vec{\sigma}_1\cdot\vec{\sigma}_2$ terms play a more important role. Some of the $\bar{N}N$ spin parameters can be measured in the upcoming experiments at LEAR. We look forward to these data, which should enable us to make considerable progress in achieving a unified description of the NN and $\bar{N}N$ interactions.

*Permanent address: Laboratoire de Physique Théorique des Particules Elémentaires et Institut de Physique Nucléaire, Division de Physique Théorique, Tour 16, ler étage, 4 Place Jussieu, 75230 Paris Cedex 05, France.

[1]M. Ceshia, Phys. Rev. D 2, 2555 (1970); T. Ohsugi *et al.*, Nuovo Cimento 17 A, 456 (1973).

[2]T. Ueda, Prog. Theor. Phys. 62, 1670 (1979); this paper gives references to data on $\bar{N}N$ differential cross sections and polarization.

[3]V. Flaminio *et al.*, CERN-HERA Report 79-03, 1979.
[4]O. D. Dalkarov and F. Myrher, Nuovo Cimento A 40, 152 (1977).
[5]C. B. Dover and J. M. Richard, Ann. Phys. (N.Y.) 121, 70 (1979).
[6]For several reviews of the LEAR project, see *Proceedings of the 5th European Symposium on Nucleon-Antinucleon Interactions, Bressanone, 1980* (CLEUP, Padua, 1980), articles by G. Plass, U. Gastaldi, and K. Kilian.
[7]W. N. Cottingham, M. Lacombe, B. Loiseau, J. M. Richard, and R. Vinh Mau, Phys. Rev. D 8, 800 (1973); M. Lacombe, B. Loiseau, J. M. Richard, R. Vinh Mau, P. Pires, and R. de Tourreil, *ibid.* 12, 1495 (1975).
[8]R. Vinh Mau, in *Mesons in Nuclei,* edited by M. Rho and D. Wilkinson (North-Holland, Amsterdam, 1978).
[9]W. Buck, C. B. Dover, and J. M. Richard, Ann. Phys. (N.Y.) 121, 47 (1979).
[10]C. B. Dover and J. M. Richard, Phys. Rev. C 21, 1466 (1980); see also the earlier work on the optical model approach by R. A. Bryan and R. J. N. Phillips, Nucl. Phys. B5, 201 (1968).
[11]See, e.g., R. Vinh Mau, Proceedings of the Ninth International Conference on High Energy Physics and Nuclear Structure, Versailles, France, 1981, Nucl. Phys. A (to be published); see also contributed paper by J. Coté, M. Lacombe, B. Loiseau, B. Moussalem, and R. Vinh Mau to this conference.
[12]A. Martin, Phys. Rev. 124, 614 (1961).
[13]M. Maruyama and T. Ueda, Nucl. Phys. A364, 297 (1981).
[14]R. A. Freedman, W. -Y. P. Hwang, and L. Wilets, Phys. Rev. D 23, 1103 (1981).
[15]N. Hoshizaki, Suppl. Prog. Theor. Phys. 42, 107 (1968).
[16]J. Bystricki, F. Lehar, and P. Winternitz, J. Phys. 39, 1 (1978).
[17]J. M. Richard, *Proceedings of the International Symposium on High Energy Physics with Polarized Beams and Polarized Targets, Lausanne, 1980,* edited by C. Joseph and J. Soffer (Birkauser, Basel, 1980). Note that A_t and A_t' have the wrong sign in this paper.
[18]K. Kilian and L. Dick *et al.*, in Ref. 17.
[19]K. Kilian, H. Poth, and J. M. Richard, CERN Report CERN/PSCC/81-46, 1981.
[20]M. Bodganski *et al.*, Phys. Lett. 62 B, 117 (1976).
[21]H. Becker *et al.*, Nucl. Phys. B141, 48 (1978); B. Jayet *et al.*, Nuovo Cimento 45 A, 371 (1978).
[22]P. D. Barnes *et al.*, CERN Report CERN/PSCC/81-69, 1981; see also Ref. 18.